AD-A099 815 IMPERIAL COLL OF SCIENCE AND TECHNOLOGY LONDON (ENGLAND) F/G 11/6
ELEVATED TEMPERATURE AQUEOUS STRESS-CORROSION OF STAINLESS STEE--ETC(U)
FEB 81 M G LACKEY, H M FLOWER, F J HUMPHREYS DAJA37-80-M-0046

UNCLASSIFIED NL

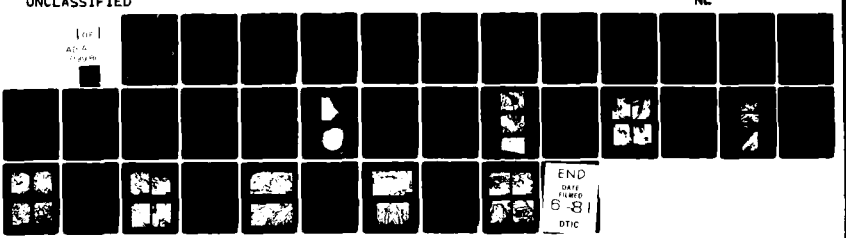

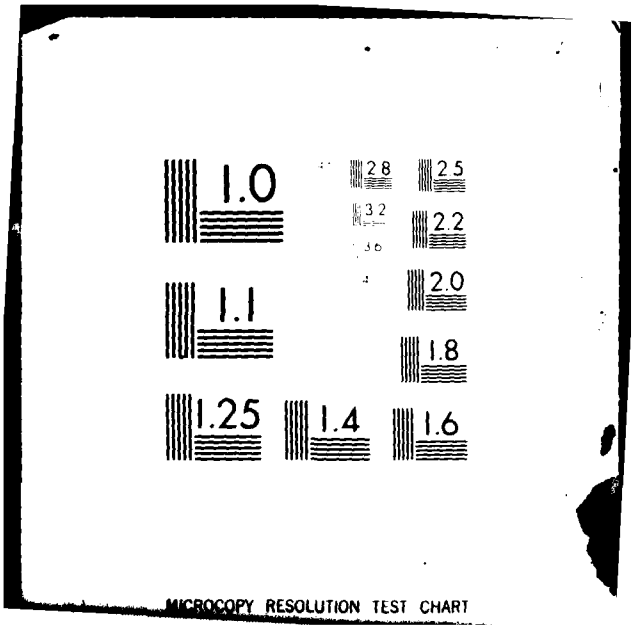
1.0
2.8
2.5
3.2
2.2
2.0
1.1
1.8
1.25
1.4
1.6
MICROCOPY RESOLUTION TEST CHART

UNCLASSIFIED
SECURITY CLASSIFICATION OF THIS PAGE (When Data Entered)

LEVEL II

LS

R&D 2821A-MS

12

REPORT DOCUMENTATION PAGE

READ INSTRUCTIONS BEFORE COMPLETING FORM

1. REPORT NUMBER	2. GOVT ACCESSION NO. AD-A099 815
3. RECIPIENT'S CATALOG NUMBER	
4. TITLE (and Subtitle) Elevated Temperature Aqueous Stress-Corrosion of Stainless Steel	5. TYPE OF REPORT & PERIOD COVERED Final Technical Report Apr 80 - Dec 80
	6. PERFORMING ORG. REPORT NUMBER
7. AUTHOR(s) M.G. Lackey, H.M. Flower and F.J. Humphreys	8. CONTRACT OR GRANT NUMBER(s) DAJA37-80-M-0046
9. PERFORMING ORGANIZATION NAME AND ADDRESS Imperial College of Science and Technology, Prince Consort Road London (England)	10. PROGRAM ELEMENT, PROJECT, TASK AREA & WORK UNIT NUMBERS 6.11.02A 1T161102BH57-04
11. CONTROLLING OFFICE NAME AND ADDRESS USARDSG-UK Box 65, FPO NY 09510	12. REPORT DATE Dec 80
	13. NUMBER OF PAGES 32
14. MONITORING AGENCY NAME & ADDRESS (if different from Controlling Office)	15. SECURITY CLASS. (of this report) Unclassified
	15a. DECLASSIFICATION/DOWNGRADING SCHEDULE

AD A099815

16. DISTRIBUTION STATEMENT (of this Report)

Approved for Public Release: distribution unlimited

DTIC ELECTE JUN 0 8 1981 S D E

17. DISTRIBUTION STATEMENT (of the abstract entered in Block 20, if different from Report)

18. SUPPLEMENTARY NOTES

19. KEY WORDS (Continue on reverse side if necessary and identify by block number)

Austenitic stainless steel
Sensitisation
Intergranular cracking
Hydrogen embrittlement

20. ABSTRACT (Continue on reverse side if necessary and identify by block number)

The susceptibility of sensitised austenitic 304 stainless steel to aqueous or dilute acid attack at ambient and elevated temperatures has been investigated. It is found that, unlike aluminium alloys, this material under the conditions investigated is not embrittled by pre-exposure to water vapour and it is concluded that this is due to the inability of hydrogen to permeate the oxide surface film during static testing.

Next page

Contd.....

DD FORM 1 JAN 73 1473 EDITION OF 1 NOV 65 IS OBSOLETE

UNCLASSIFIED
SECURITY CLASSIFICATION OF THIS PAGE (When Data Entered)

20. Contd.

Slow strain rate testing in dilute acid, under free corrosion or cathodic potential, has shown that hydrogen embrittlement is an important factor in the intergranular stress corrosion cracking of austenitic stainless steel.

Cathodic charging of thin foils with hydrogen was found to promote the formation on martensite and intergranular cracks.

(6) ELEVATED TEMPERATURE AQUEOUS STRESS-CORROSION OF STAINLESS STEEL.

(9) Annual Technical Report. (Final) Apr-Dec 61

by

(10) M.G. Lackey, H.M. Flower and F.J. Humphreys

(11) Feb [redacted] 61

(12) 34

European Research Office,

United States Army

London England.

(15) Grant No DAJ A37-80-M-0046

(16) 1T161102...

Imperial College

(17) ...

Approved for Public Release: distribution unlimited.

ABSTRACT

The susceptibility of sensitised austenitic 304 stainless steel to aqueous or dilute acid attack at ambient and elevated temperatures has been investigated. It is found that, unlike aluminium alloys, this material under the conditions investigated is not embrittled by pre-exposure to water vapour and it is concluded that this is due to the inability of hydrogen to permeate the oxide surface film during static testing.

Slow strain rate testing in dilute acid, under free corrosion or cathodic potential, has shown that hydrogen embrittlement is an important factor in the intergranular stress corrosion cracking of austenitic stainless steel.

Cathodic charging of thin foils with hydrogen was found to promote the formation on martensite and intergranular cracks.

1. INTRODUCTION.

This is a final report of the work carried out under Grant No. DAJ A37-80-M-0046. The research is aimed particularly at investigating the effect of hydrogen on the stress-corrosion behaviour of sensitised austenitic stainless steels, and is a continuation of the project funded under Grant No. DA-ERO-72-G-011. Three different types of test have been carried out. These are: pre-exposure testing, slow strain rate testing under a cathodic potential and the examination of cathodically charged thin foils.

2. PRE-EXPOSURE TESTING.

As the existence of "pre-exposure" embrittlement of Al-Zn-Mg alloys in water vapour has been well documented (see DA-ERO-77-G-011) it was thought that a similar mode of hydrogen embrittlement may occur in sensitised stainless steel. In order to determine whether this was the case, "in-situ" experiments were conducted on sensitised specimens using the Gas Reaction cell (GRC) in the AEI-7 HVEM. Sensitised specimens were also tested in a specially designed steam cell.

2.1 Gas Reaction Cell.

The GRC provides a unique opportunity to study gas-metal reactions in the electron microscope. The cell employed in this investigation is a Swann, differentially pumped, aperture-limited cell. A gas reservoir of approximately 500ml capacity is created near the specimen between the upper and lower pole pieces. The pressure within the cell can be varied.

For the experiments on type 304 steel, strained and unstrained TEM specimens were used. The cell environment was water-saturated He at 20°C at a pressure of ~ 100 torr. Experiments were performed at 500 kV and 1 MeV. Video facilities were available for filming the reaction. Sensitised specimens, prepared by the technique described in earlier reports, were examined in the as-heat-treated or as-deformed condition. By studying the deformed material, the influence of the 'grain boundary' martensite on any hydrogen-metal reaction could be evaluated.

The results of the "in-situ" GRC experiments revealed that no microstructural changes occurred when the specimens were exposed to H_2O vapour environments. Only a small degree of surface reaction was observed as depicted in Figure 1. There was no preferential reaction at the grain boundary regions in either the strained or the unstrained material for exposure times up to 30 minutes. The accelerating voltages used for these experiments were 500 kV and 1 MeV. Increasing the accelerating voltage promoted radiation damage of the metal. The extent of the radiation damage induced in a sensitised specimen is illustrated in Figure 2.

2.2 High Temperature Steam Cell.

The susceptibility of sensitised austenitic stainless steel to intergranular cracking in BWR cooling pipes prompted further study into H_2O vapour as an SCC/HE environment. It was not possible in this investigation to simulate accurately the conditions in BWR cooling pipes: H_2O at 343°C. Therefore an apparatus was built which enabled the specimens to be exposed

to superheated dry steam at atmospheric pressure.

The cell (Figure 3) consisted of a 30 mm diameter quartz tube (sealed at one end) which was inserted in a tube furnace. The open end of the quartz tube, which extended ~1 cm outside the furnace, was sealed with a silicon rubber bung. Two 4.0 mm diameter pyrex tubes inserted into the furnace enabled the steam to pass over the specimens in the quartz tube. The tube inlet was considerably longer than the outlet tube (located in the cool end of the cell so that the steam would attain furnace temperature before reaching the specimens. The outgoing steam was carried via the outlet tube to a reflux condensor. As the steam condensed, it was collected in a funnel and fed back to the steam source (water-filled flask on hot plate). A thermocouple was inserted into the quartz tube so that the temperature of the steam cell could be monitored. The temperature during the tests was approximately 320°C.

Three types of specimen were used for these experiments: unstressed, stressed and pre-strained (5% E). All specimens were electropolished prior to testing. The specimens tested under stress were U-bend specimens, held in a stainless steel clamping device (a Type 304 stainless steel threaded bolt and 2 Type 304 threaded discs).

Initial results of mechanical properties of sensitised specimens 'pre-exposed' to steam at 120°C (pressure of 2.06 bars) for 90 days revealed no decrease in ductility nor any fractographic evidence of hydrogen embrittlement. As conditions in BWR environments (343°C H_2O) are more severe than those in the 120°C autoclave, it was decided to "pre-expose" specimens in steam at 320°C and one atmosphere pressure. The steam cell, described above, was designed to accommodate "pre-exposure" and "U-bend" type tests in high temperature, dry steam.

No embrittlement was detected for any specimens tested at 340°C for

prolonged periods (40 days). All specimens, unstressed or pre-strained, failed in a ductile manner. Typical fracture morphologies are presented in Figure 4. Micrograph A depicts the type of fracture in the unstressed specimens, while B and C represent the pre-strained material. Intergranular tearing, characteristic of ductile failure in an inert environment, occurred in addition to dimpling. Micrograph C illustrates a region of intergranular tearing caused by the presence of carbides at the grain boundaries.

2.3 Discussion of "Pre-exposure" Results

Austenitic stainless steel is susceptible to hydrogen embrittlement in the solution annealed or sensitised condition. In this investigation however, no embrittlement effects have been detected in specimens which were pre-exposed to water vapour. Although numerous examples of intergranular cracking of sensitised 304 in BWR environments have been reported in the literature, due to the inability to obtain the high temperature (288^{o}C) and high pressure ($\sim$ 100 atm) H_2O environment in the laboratory, it was not possible to duplicate the BWR conditions.

Two important factors which may account for the low reactivity of the metal with water vapour in the laboratory test conditions are the hydrogen fugacity and the presence of the oxide film on stainless steel.

2.3.1 Hydrogen Fugacity.

Austenitic stainless steel can become enbrittled when tested in hydrogen gas or by the introduction of hydrogen electrolytically (cathodic charging). Briant (1) has recently reported instances of hydrogen-assisted cracking of sensitised Type 304 steel in one atmosphere of H_2. This is equivalent to a hydrogen fugacity of 1. The hydrogen fugacity can also be increased by cathodically charging the steel. Introduction of hydrogen into the steel in this manner results in embrittlement.

In the high temperature steam cell, sensitised specimens were exposed to 320°C dry steam at one atmosphere. Thermodynamic calculations indicate that the partial pressure of H_2 is equilibrium with H_2O under these conditions in approximately 10^{-38} atm. This corresponds to a comparably low fugacity of hydrogen. It is anticipated that the hydrogen fugacity in the GRC is substantially lower than that in the steam cell. These values are significantly lower then the values of the hydrogen activity calculated for the stress corrosion test conditions. If the reactivity of hydrogen with the metal is dependent upon fugacity, then the observed behaviour is consistent with the role of hydrogen fugacity in embrittlement.

2.3.2 Oxide Film.

The oxide film formed on austenitic stainless steel is an effective barrier to hydrogen penetration (2). This is particularly so in a pre-exposure test where film rupture due to straining cannot occur. Piggott and Siarkowski (2) have shown that the diffusivity of hydrogen in the oxide is very dependent upon composition, with films of α-Fe_2O_3 having a much lower D_H (1×10^{-18} cm^2/sec) than Cr_2O_3($9.2 \times .0^{-16}$ cm^2/sec). The hydrogen diffusivity (in the oxide) was observed to change with increasing thickness as a result of compositional variations in the oxide.

Oxide films approximately 1000Å or less in thickness were most effective in inhibiting the flux of hydrogen through the oxide. Piggott and Siarkowski noted that the hydrogen flux through thick (> 1000Å) oxide films was very similar to results obtained on clean metal, indicating that cracking of the oxide had occurred. The importance of the oxide film in hydrogen permeation studies was also reported by Louthan and Derrick (3). Electropolished stainless steels were more effective in reducing hydrogen permeation than were mechanically polished specimens. Exposure of austenitic stainless steel to water vapour resulted in a dramatic reduction of hydrogen permeability.

The experimental observations regarding the influence of hydrogen

on the microstructure and properties of sensitised 304 can be readily explained by the low hydrogen fugacity and the inhibiting effect of the oxide film (particularly in wet environments) on hydrogen permeation. Hydrogen introduced by cathodic charging techniques did induce microstructural changes. The absence of any hydrogen-effects in the "pre-exposure" tests indicates that very little hydrogen - if any - could enter the metal.

3. EFFECT OF CATHODICALLY-PRODUCED HYDROGEN ON THE MICROSTRUCTURE OF SENSITISED TYPE 304 STEEL.

Numerous studies have been conducted on cathodically-charged solution annealed type 304 steel to determine the effect of dissolved hydrogen on the microstructure and mechanical behaviour (e.g. (4)). It has been reported that the presence of hydrogen leads to severe internal stresses in the austenite (5,6) and can induce the $\gamma \rightarrow \varepsilon$ or $\gamma \rightarrow \alpha'$ transformation. Hydrogen also reduces the stacking fault energy in austenitic stainless steels (7).

The microstructural effect of hydrogen in sensitised austenitic stainless steel was evaluated through examination of cathodically charged specimens. Electrolytic charging was conducted in a 2 vol % H_2SO_4 solution, containing 250 mg/ℓ of sodium arsenate as a hydrogen recombination poison. Thin foil specimens were charged for periods of 3 to 15 min. at a current density of approximately 70 mA/cm^2 at 25°C. Examination of the charged specimens in the transmission electron microscope revealed extensive faulting and twinning of the austenite (Fig. 5A). This rather high degree of deformation induced the transformation of $\gamma \rightarrow \alpha'$ at many grain boundaries (Micrograph B). Regions of ε martensite were observed in the γ after charging (Micrographs A and C). In addition to the deformation structures, intragranular cracking was detected (Micrograph D). The cracks were crystallographic in nature and appear to grow in <111> directions. The observed crack morphology and crystallography are remarkably similar to the slotted dissolution morphology observed by Scamans in studies

of SCC initiation in LiCl (8).

3.1 Discussion of cathodic charging results.

The primary objective of cathodically charging sensitised specimens with hydrogen was to determine whether the stresses involved in introducing hydrogen into the metal would be sufficient to promote the $\gamma \rightarrow \alpha'$ and $\gamma \rightarrow \epsilon$ transformations. This was successfully accomplished.

An additional feature of cathodic charging at room temperature is the formation of fine, crystallographic, intragranular cracks in the austenite. This preliminary study indicates that these cracks are not related to α' or ϵ martensite, but may be due to hydrogen embrittlement of the austenite, a view shared by other investigators (138,207). The similarity of the crack morphology + crystallography with the dissolution attack observed by Scamans (61) in his investigation on SCC of austenitic stainless steels in 150°C LiCl, suggests that the two types of attack may be related. It is possible, of course, that hydrogen cracking and dissolution proceed in the same mode in this system. Clearly, this area requires further investigation.

4. SLOW STRAIN RATE TESTS CONDUCTED UNDER CONTROLLED CATHODIC POTENTIAL

For hydrogen embrittlement models of SCC, crack propagation should be enhanced under cathodic potentials. Therefore, to elucidate the primary mechanism of stress corrosion cracking (propagation), stress corrosion tests were conducted under potential control, at a strain rate of 2×10^{-6} sec^{-1}.

A series of sensitisation treatments were examined (2,24 and 72 hours at 675°C) in two solutions (0.1 M H_2SO_4 + 0.02 M NaCl (pH=1), and 0.01 M H_2SO_4 + 0.002 M NaCl (pH=2) under a cathodic potential of -650 mV (SCE) which is approximately 200 mV from the corrosion potential of the low chromium material at the sensitised grain boundaries.

4.1 Results.

All sensitised specimens failed prematurely when tested in either solution under cathodic polarisation (-650mV SCE). (Table 1) Examination of the fracture surfaces revealed regions in intergranular and cleavage-like fracture, representative fractographs of which are presented in Figs. 6-8.

The primary fracture mode in the 72 hour specimens was intergranular, with cleavage-like regions becoming more prominent as the sensitisation time decreased. Micrograph A in Figure 6 is typical of the 72 hour specimens. Indications of hydrogen cracking are evident in Micrograph B where fine transgranular cracks can be detected on a carbide-covered intergranular face. The absence of dissolution attack is demonstrated in Micrograph C which contains a high magnification micrograph of an intergranular crack. Depressions can be seen on the grain where once carbides had been present.

Specimens sensitised for 24 hours exhibited similar behaviour when tested under cathodic potential. Two fracture modes - intergranular and cleavage-like - characterised these failures. Strains to failure were slightly greater than those for the 72 hour specimens. Slip lines are visible in the intergranular region portrayed in Micrograph A in Figure 7. Individual carbides were still easily resolved (Micrograph B). Representative micrographs of fracture surfaces examined after testing in the pH=1 and pH=2 solutions, are presented in Micrographs C and D respectively. Some slip line attack can be observed in Micrograph C. No difference in strain to failure was detected for these specimens.

The greatest failure strains were associated with the specimens sensitised for 2 hours. Once again, the fracture surface was characterised by regions of intergranular and cleavage-like failure, as illustrated in Fig. 8 (Micrograph A). Secondary cracking on an intergranular face is shown in Micrograph B. The cracking is crystallographic, as would be expected for the case of hydrogen cracking. Micrographs C and D contain additional

examples of transgranular fracture. It appears to be crystallographic and fine in structure.

Fracture matching was undertaken in order to confirm that the cleavage-like fracture was not related to slip but rather due to embrittlement. Micrographs of matched fracture surfaces are presented in Figures 9 and 10. Also included in Figure 9 are two matching micrographs of the cleavage-like fracture; one micrograph is reverse-printed so that a detailed comparison of the features may be made. The second set of matched micrographs (Fig. 10) depicts the effect of the acid environment on the fine, cleavage-like structure. The left fracture surface was kept under cathodic control. The opposite face however was not cathodically protected after fracture and was permitted to corrode freely for approximately 3 hours. A small amount of attack occurred, and corrosion product can be readily detected in the right micrograph.

All slow strain rate tests conducted under cathodic potential displayed similar fracture morphologies. The strains to failure for each sensitisation treatment paralleled those results obtained under free corrosion conditions in that the 72 hour specimens fractured at the lowest strain, while the 2 hour specimens failed at the highest value (ε_f = 0.22).

Characteristic fracture surfaces of specimens which had failed after slow strain rate testing without an applied potential are shown in Fig. 11. The fracture surfaces were predominantly intergranular, (A and B), but areas of a "feathery" type of fracture, sometimes termed "quasi-cleavage", were also observed (C).

4.2 Discussion.

Material susceptible to hydrogen embrittlement would be expected to fail prematurely under cathodic polarisation, while that susceptible to dissolution would fail less readily. It can be seen from Table 1 that there is in general a substantial decrease in ductility for the specimens tested under cathodic conditions, suggesting that hydrogen embrittlement

plays an important role in the stress corrosion process. The fractographic evidence also reveals a strong similarity between free corrosion failures and cathodic failures.

It is proposed that the stress corrosion cracking of sensitised 304 steel in dilute H_2SO_4 + NaCl solutions proceeds as follows.

In the acidic environment, initial dissolution attack occurs at sensitised grain boundaries as a result of the chromium depletion, leading to the formation of a pit. The pits act as stress concentrators and, as the stress increases, the grain boundary material is transformed to a narrow band of α' martensite. The acidic solution containing Cl^- ions breaks down the passive film in the pit, thereby permitting hydrogen to enter the metal. Hydrogen entry is also enhanced by the increased hydrogen activity at the crack tip due to the beneficial effect of the Cl^- ions (9).

Once hydrogen is absorbed and is accumulated in the plastic zone (in which is located the sensitised grain boundary), the strain-induced martensite fractures along the grain boundary which is the weakest link in the metal. The crack advances but blunts as it enters the unembrittled material. As the stress increases, hydrogen will segregate preferentially in the plastic zone (particularly in the martensite) and, upon attaining the critical hydrogen concentration, the crack advances once again. The transition from inter to transgranular cracking can be explained in view of the results of Hänninen et al (10) in that the austenite or ε martensite may become embrittled. The observation that fracture is predominantly intergranular rather than transgranular in sensitised austenitic stainless steels is dependent upon the existence of α' in the chromium-depleted zone.

5. CONCLUSIONS

1. In this investigation it has been shown that hydrogen embrittlement is the mechanism of stress corrosion cracking of sensitised type 304 stainless steel in dilute H_2SO_4 + NaCl solutions. Although it is possible for dissolution to occur in these solutions, it appears to be of secondary importance, with the crack advancing as the result of hydrogen embrittlement.

2. Austenitic stainless steels are not prone to "pre-exposure" embrittlement effects in dry steam at 343°C (1 atm). "In situ" observations in the Gas Reaction Cell in the HVEM did not reveal any preferential reaction of the H_2O vapour with the metal. No H_2 bubble formation was observed at the sensitised grain boundaries.

3. Cathodically charging sensitised thin foils with hydrogen promoted the $\gamma \rightarrow \alpha' + \varepsilon$ transformation, and resulted in the formation of crystallographic intragranular cracks in the austenite.

TABLE 1

Sensitisation at 675°C	True strain to failure	
	Free corrosion	Cathodic potential
2hrs	0.45	0.22
24 hrs	0.42	0.17
72 hrs	0.12	0.13

Strain to failure for specimens in pH 2 solution.

REFERENCES

1. C.L. Briant, Met. Trans., 9A (1978) p.731.
2. M.R. Piggott and A.C. Siarkowski, JISI, 210 (1972) p. 901
3. M.R. Louthan and R.G. Derrick, Corros. Sci., 15 (1975) p. 565
4. K. Kamachi, M. Oka and M. Touge, Proc. 1st Int. Symp. on New Aspects of Martensitic Transformation: Trans. JIM, 17 (1976) p. 309.
5. M.L. Holzworth and M.R. Louthan, Corrosion, 24 (1968) p. 110.
6. J. Burke, A. Jickels, P. Maulik and M.I. Mehta, ref. 96, p. 102
7. P.D. Pritcher, Ph.D. Thesis, University of Wales, 1979.
8. G.M. Scamans, Ph.D. Thesis, Imperial College of Science & Technology, Univ. of London, 1974.
9. J. McBreen and M.S. Grenshaw, Fundamental Aspects of SCC, ed. R.W. Staehle (NACE 1969) p. 51.
10. H. Hänninen and T. Hakkarainen, Corrosion, 36 (1980) p. 47.

Figure 1. Micrograph of Sensitised Specimen After Exposure for 10 Minutes in the GRC.

Figure 2. Radiation Damage After 20 Minutes Exposure in the GRC (operating voltage = 1 MeV)


0.5µm

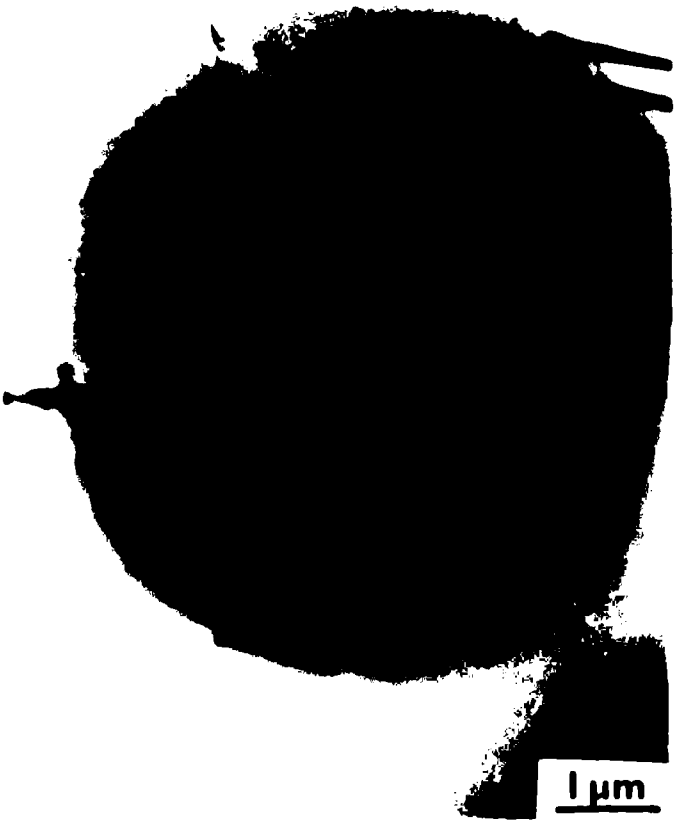
1µm

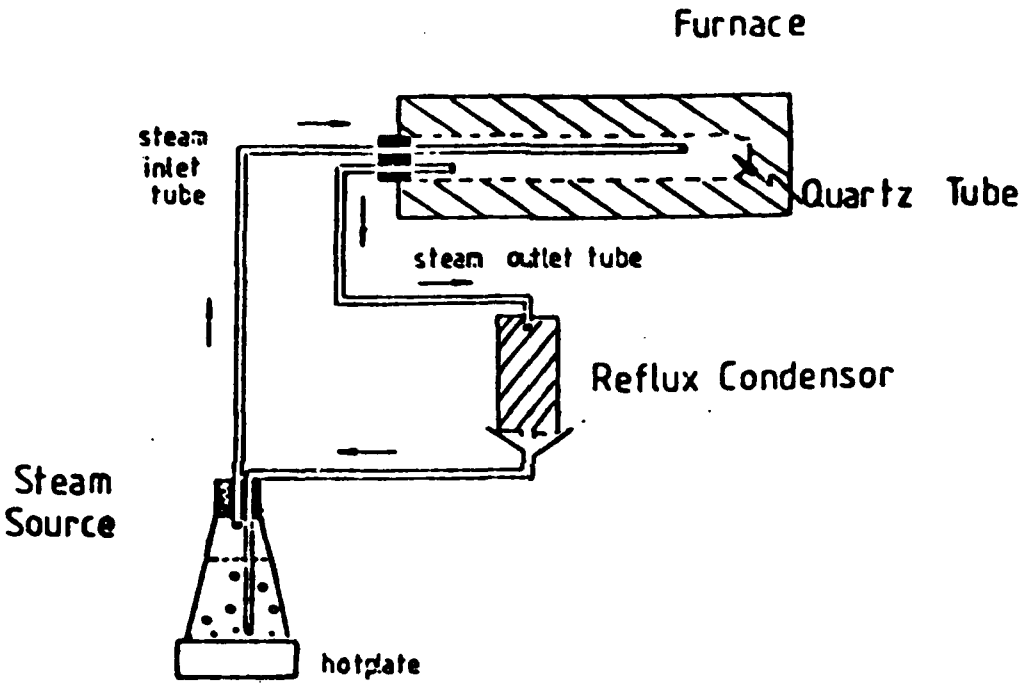

Figure 3. Schematic Diagram of High Temperature Steam Cell

Figure 4 . Representative Fractographs of Sensitised Specimens Tested After Exposure to Dry Steam (340°C) for 40 Days.

A) Sensitised for 2 hrs. @ 675°C

B) Sensitised for 24 hrs. @ 675°C

C) ensitised for 72 hrs. @ 675°C


A
20µm


B
20µm

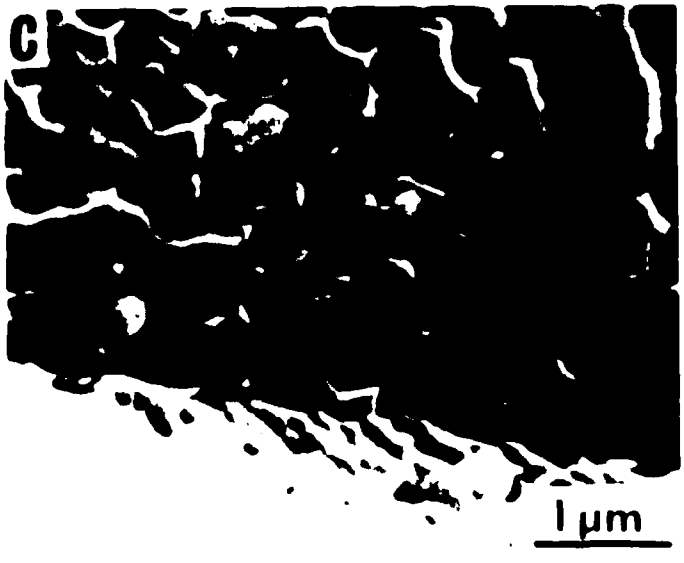
C
1µm

Figure 5. Representative Micrographs of Heavily Sensitised Specimens (72 hrs. @ 675°C) After Cathodic Charging at 25°C .

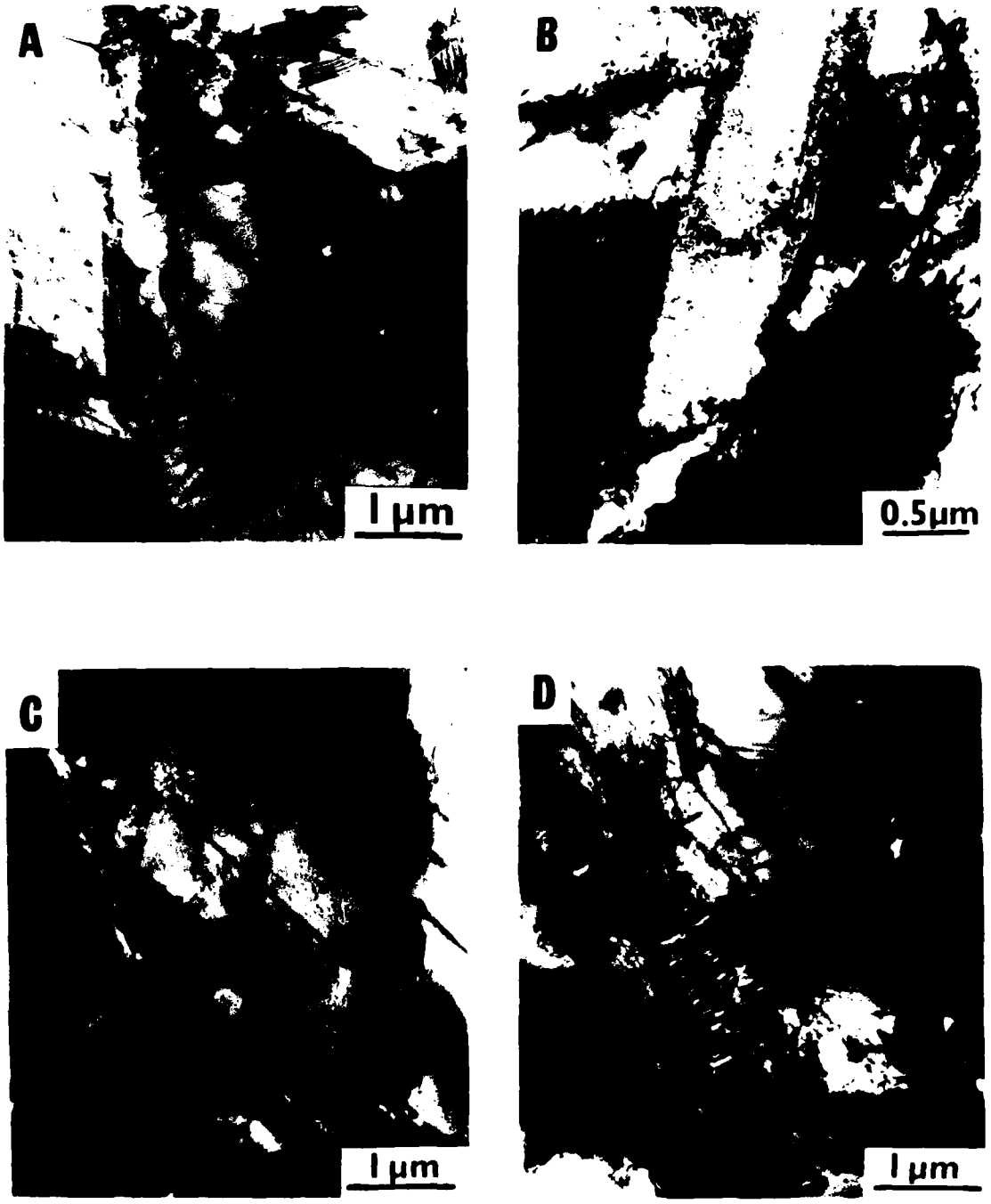
A
1 µm
B
0.5µm
C
1 µm
D
1 µm

Figure 6. Representative Fractographs of Sensitised Specimens (72 hrs. @ 675 ^{o}C) Tested in pH=2 0.01M H_2SO_4 + 0.002M NaCl Solution Under Cathodic Control (-650 mV SCE)

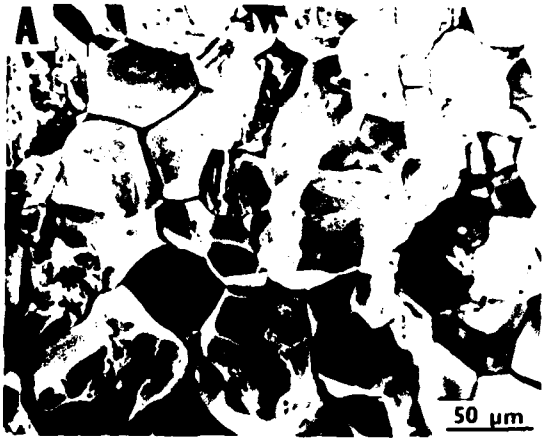
A
50 µm

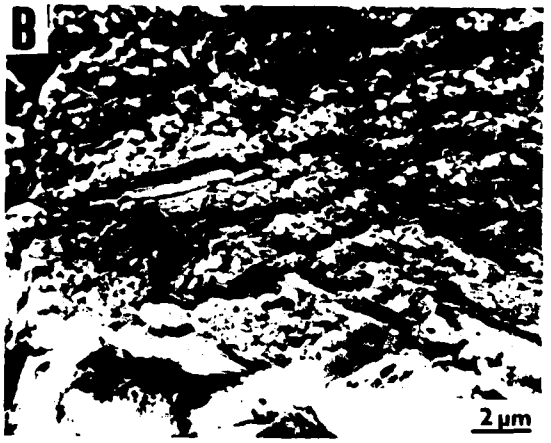
B
2 µm


C
1 µm

Figure 7. Representative Fractographs of Specimens Sensitised for 24 hrs. @ 675 °C Tested Under Cathodic Control in:
A,B,D) pH=2 0.01M H_2SO_4 + 0.002M NaCl
C) pH=1 0.1M H_2SO_4 + 0.02M NaCl


A
10 µm


B
0.5µm


C
50 µm


D
10 µm

Figure 8. Representative Fractographs of Specimens Sensitised for 2 hrs. @ 675 ^{o}C and Tested Under Cathodic Control (-650 mV SCE)

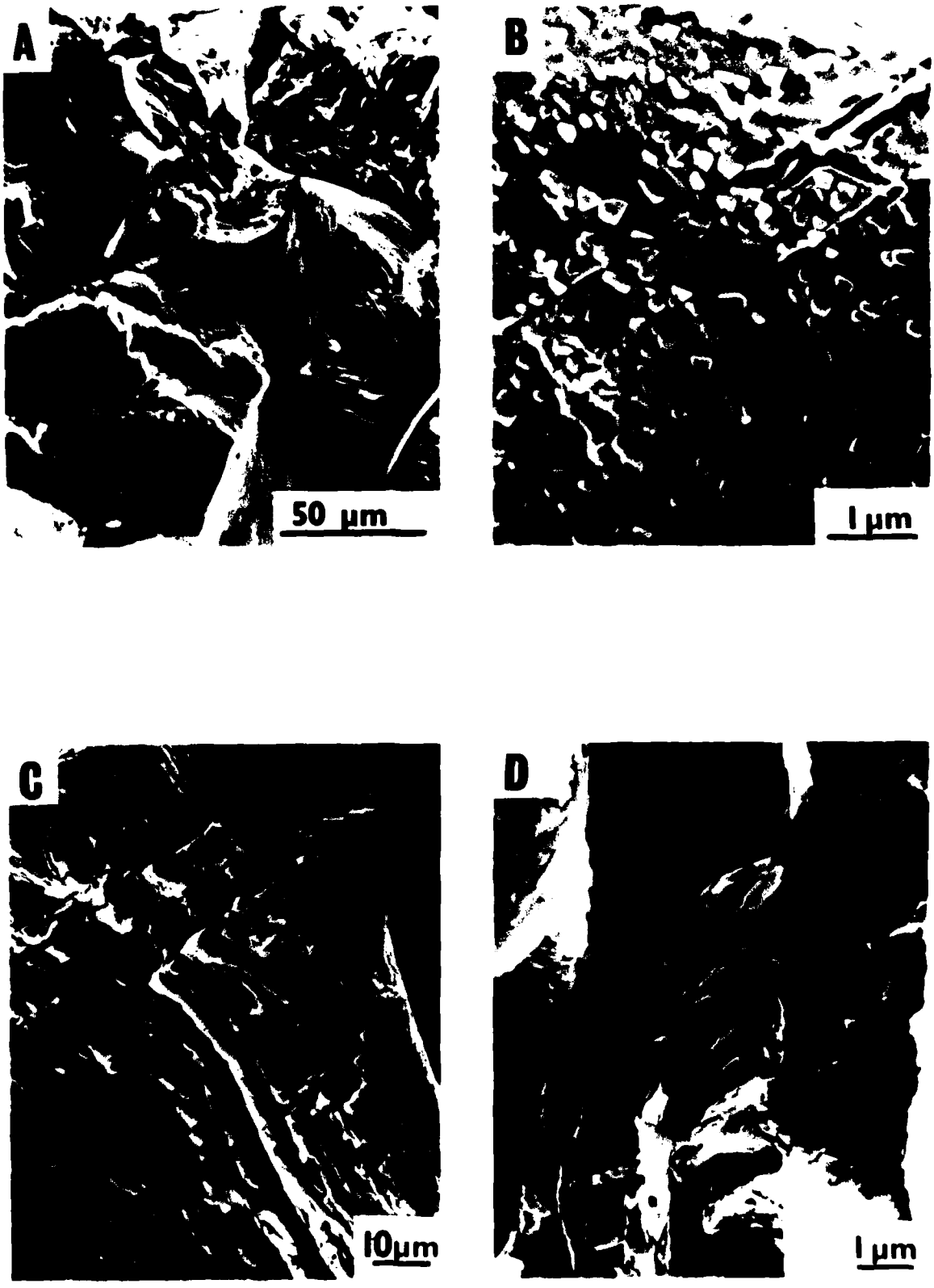
A
50 µm
B
1 µm
C
10µm
D
1 µm

Figure 9. Matching Fracture Surfaces From Sensitised Specimens (24 hrs. @ 675°C) Tested in pH=2 0.01M H_2SO_4 + 0.002M NaCl Solution Under Cathodic Control (-650 mV SCE). The lower right-hand micrograph is reverse printed to enable a comparison of the features to be made.


50 µm

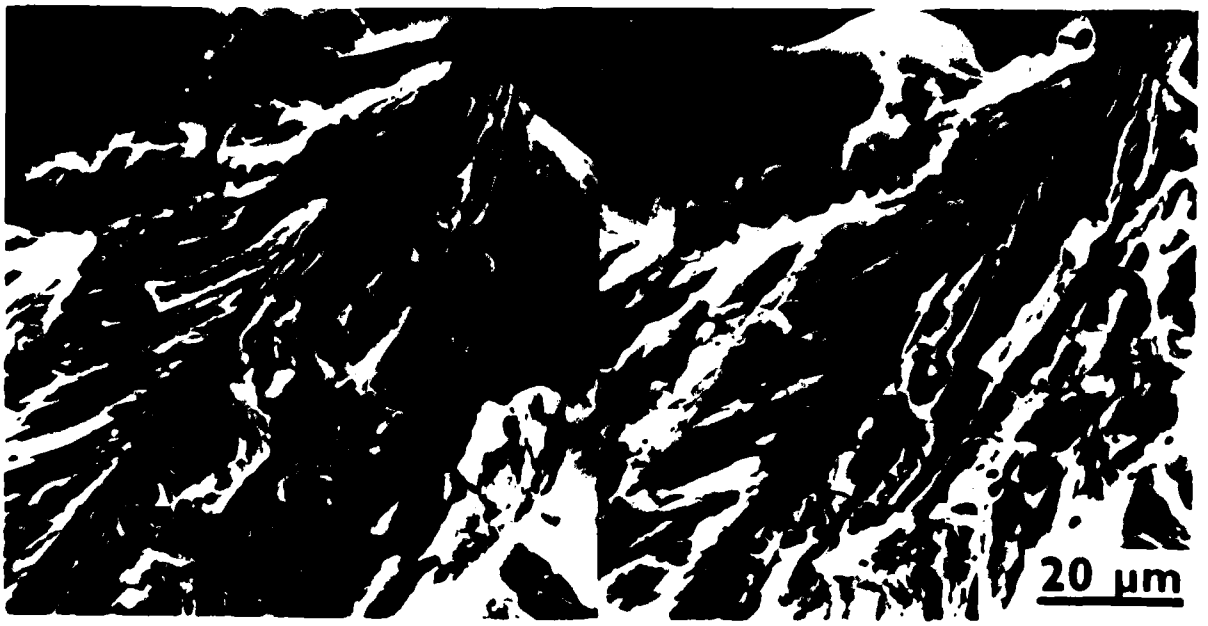
20 µm

Figure 10. Matching Fracture Surfaces From Sensitised Specimens (24 hrs. @ 675°C) Tested in pH=2 0.01M H_2SO_4 + 0.002M NaCl Solution Under Cathodic Control (-650 mV SCE).
The effect of post-fracture dissolution can be observed in the lower micrographs. The surface on the left was exposed to the solution while under cathodic protection, while that on the right was permitted to corrode freely.

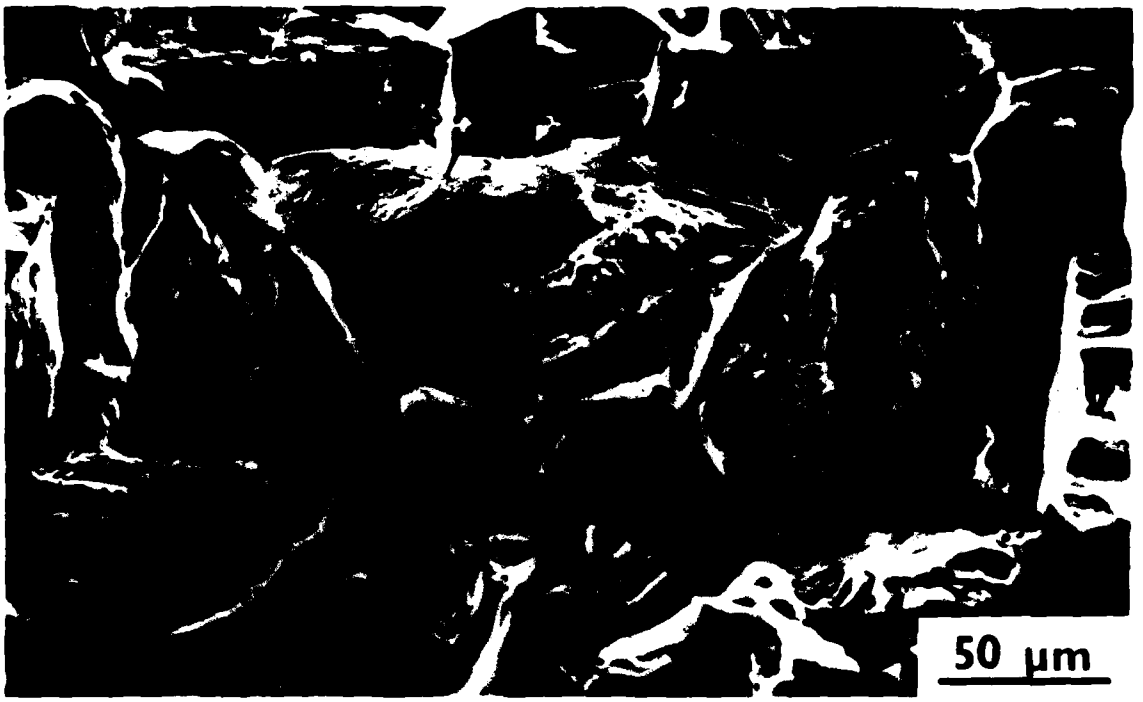
50 µm


10 µm

Figure 11. Representative Fractographs of Sensitised (72 hrs. @ 675 °C) Specimens Stress Corroded in pH=1 0.1M H_2SO_4 + 0.02M NaCl Solution.

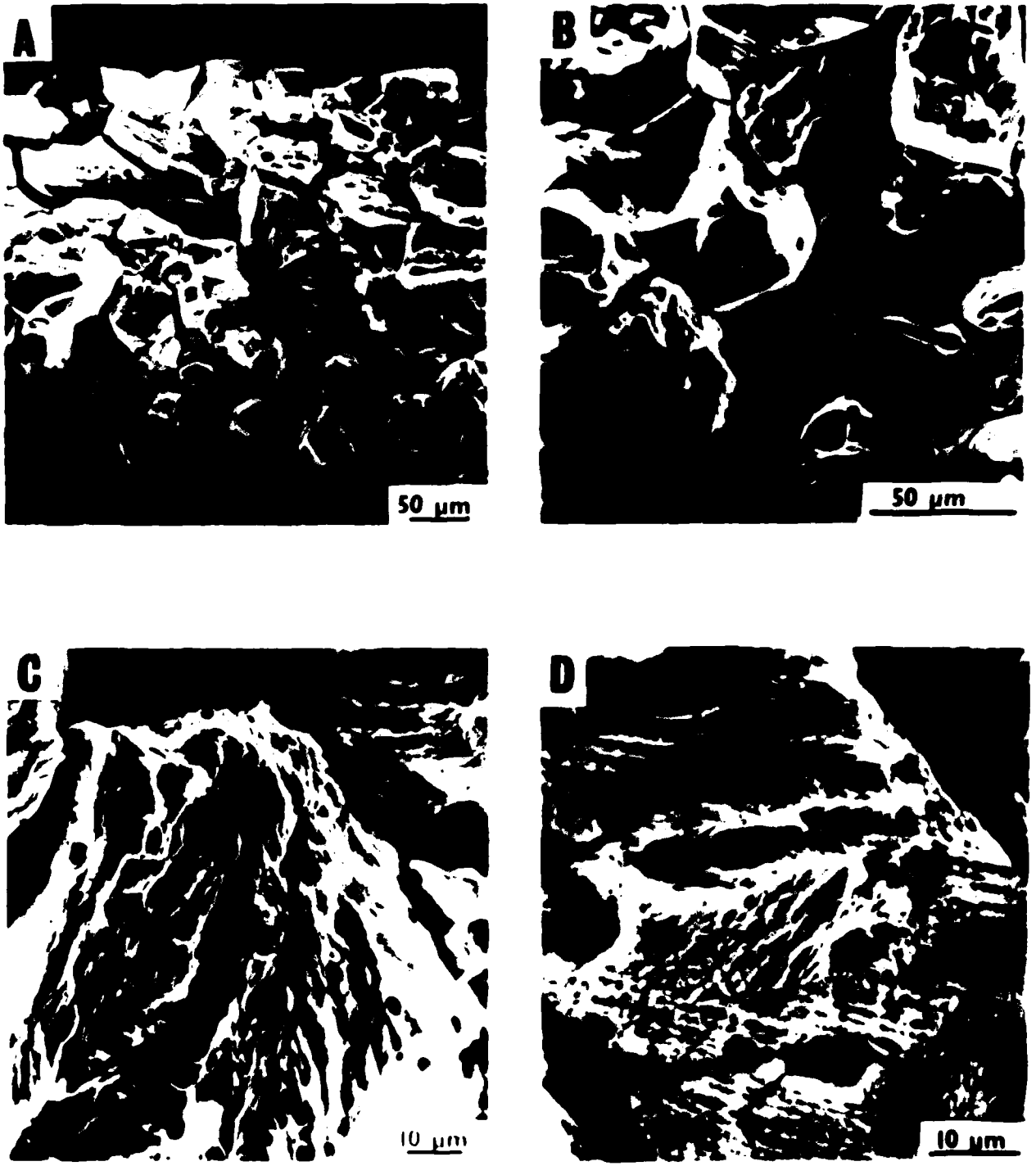
A
50 µm
B
50 µm
C
10 µm
D
10 µm

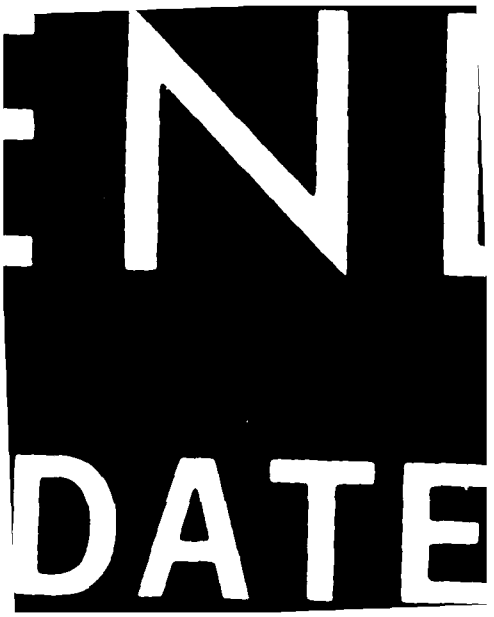
N
DATE